Local Temperature Sensitivity Coefficients of a Deterred Spherical Single Base Gun Propellant

Karim. M. Boulkadid,[1]* **Michel. H. Lefebvre,[2]**
Laurence Jeunieau,[2] **Alain Dejeaifve[3]**

[1] *UER Chimie Appliquée, Ecole Militaire Polytechnique EMP,*
 BP 17 Bordj El-Bahri, 16046 Algiers, Algeria
[2] *Laboratory for Energetic Materials, Royal Military Academy,*
 Av. de la Renaissance 30, 1000 Brussels, Belgium
[3] *PB Clermont SA, Rue de Clermont 176, 4480 Engis, Belgium*
E-mail: karim.boulkadid@gmail.com

Abstract: In our previous investigation, we measured the global temperature sensitivity coefficient of a deterred spherical single base gun propellant following an experimental procedure that did not allows us to determine the local temperature sensitivity coefficients of the deterred and undeterred parts of the investigated propellant. In this paper, we propose an experimental methodology to measure the local temperature sensitivity coefficients of both parts of the spherical deterred gun propellant. This methodology can be summarized as follows: Firstly, we separated the ranges of pressure where the combustion of the deterred and the undeterred parts of the spherical propellant occurs by means of infrared (IR) microscopy measurements. Then the burning rate of the propellant as a function of pressure was calculated according to STANAG 4115 at different initial temperatures. Finally, we determined the local temperature sensitivity coefficients of each part of the spherical propellant.

Keywords: initial temperature, temperature sensitivity coefficient, deterred propellant, closed vessel tests, infrared microscopy

1 Introduction

The temperature sensitivity of new green formulations of gun propellants should be measured to establish their lower temperature sensitivity [1]. However, no

methodologies are available for characterizing the temperature sensitivity of gun propellants.

In a previous investigation [1], we contributed to closing this gap and to enriching the range of ballistics tests by establishing a method for the measurement of the temperature sensitivity of deterred gun propellants using a closed vessel test and ignition with black powder. In an effort to close this gap further, the present work augments the previous one and consists of the measurement of the temperature sensitivity of spherical deterred single base gun propellant using a closed vessel test and ignition with a gaseous ignition mixture.

In fact, the influence of the ignition system on the burning rate obtained has been extensively discussed elsewhere [2-6] and confirms that a closed vessel experiment with an appropriate gaseous ignition mixture (the gaseous ignition mixture used in this study) allows the combustion of the various parts of a deterred propellant to be observe. By contrast, ignition with black powder does not allow the combustion of the various parts of a deterred propellant to be observed. This results from the inhomogeneous ignition of the deterred propellant by the black powder inside a closed vessel. It is for this reason that we have been able to determine a global temperature sensitivity coefficient, despite the fact that the chemical composition of the deterred propellants investigated were not homogeneous: their surface composition was chemically modified and consisted of impregnation by a combustion rate modifier, called a "deterrent", which is only present on the surface up to a certain depth and with a certain gradient.

When a closed vessel test with a gaseous ignition mixture is employed to measure the temperature sensitivity coefficients of a deterred propellant, it is not possible to determine a global temperature sensitivity coefficient and consequently one must determine local temperature sensitivity coefficients.

Therefore, the aim of this work is to propose an experimental methodology for measuring the local temperature sensitivity coefficients of the deterred and the undeterred parts of a deterred spherical single base gun propellant. For this purpose, we employed two well know experimental procedures: infrared (IR) microscopy measurements and closed vessel tests with a gaseous ignition mixture. IR microscopy allows the ranges of pressure where the combustion of the deterred and the undeterred parts of the deterred propellant occurs to be separated. Closed vessel tests and a gaseous ignition mixture allow the burning rate of the propellant as a function of pressure according to STANAG 4115 [7], at different initial temperatures, to be determined. A specific definition of the temperature sensitivity [1] was employed in order to calculate its values at low and high temperatures, and for both deterred and undeterred parts.

2   Definitions

2.1 Initial temperature
The initial temperature, T_0, is the temperature at which the propellant is conditioned for at least for 8 h before the closed vessel tests.

2.2 Temperature sensitivity coefficient
To define the temperature sensitivity coefficient, it was assumed that in the traditional Vieille's law, $r_P = \beta \cdot P^n$, the pressure exponent, n, is not a function of the initial temperature. The temperature sensitivity coefficient $\sigma(r_P)$ of the burn rate (r) at a pressure P was thus defined as the relative change in burning rate from the value at 21 °C (benchmark temperature) resulting from a change in the initial temperature dT_0 [8-15]. The benchmark value of the propellant parameter was set at 21 °C (Equation 1).

$$\sigma(r_P) = \frac{1}{r_P(T_0 = 21°C)} \frac{dr_p}{dT_0} 100 \tag{1}$$

where:
- $\sigma(r_P)$ is the temperature sensitivity coefficient of the burning rate,
- r_P is the burning rate at pressure P.

3   Experimental Methodology

The analysis of a typical deterrent [dibutyl phthalate (DBP)] concentration profile, obtained by infrared (IR) microscopy measurement, allows three distinct zones to be observed [16]. The first zone corresponds to the deterred portion of the propellant grain, where the concentration of DBP is large. The second zone is the portion where the DBP content is lower, and the third zone contains no DBP.

The definition of the temperature sensitivity coefficient $\sigma(r_P)$ is based on the Vieille law. However this law is valid only for a homogeneous chemical composition. As already mentioned, the chemical composition of a propellant containing a deterrent is not homogeneous. Indeed, there are three parts.

Jeunieau *et al*. [2] showed that it is possible to observe the combustion of the different parts of a deterred propellant using an appropriate gaseous ignition mixture. We have employed this mixture in closed vessel tests to determine the burning rate of an investigated propellant at various initial temperatures.

After having identified the ranges of pressure where the combustion of the

three parts of the propellant occurs, we calculated the temperature sensitivity coefficient $\sigma(r_P)$ corresponding to the first and third parts, the chemically homogenous parts, in order to determine $\sigma(r_P)$ of the deterred and the undeterred parts of the propellant.

4   Propellant Investigated

A spherical single base deterred propellant was used for this investigation. The spherical propellant had an average diameter of 553 µm, and contained around 10% of nitroglycerin stabilised with diphenylamine (DPA). The average concentration of the deterrent, dibutyl phtalate (DBP), was 4.8%. The composition of the propellant is given in Table 1.

Table 1.   Composition of the investigated spherical propellant

Compound	[wt.%]
NC	81.52
H_2O	0.66
KNO_3	1.2
NGL	10.7
DBP	4.8
DPA	0.59
NDPA	0.53

NC: Nitrocellulose, NGL: Nitroglycerin, DBP: Dibutyl phthalate, DPA: Diphenylamine, NDPA: Nitrodiphenylamine.

5   Experiments and Work Programme

The deterrent concentration profile of the propellant was made visible by infrared (IR) microscopy measurements.

The determination of the propellant burning rate was performed by employing closed vessel tests and a gaseous igniter mixture; all tests were performed with the propellant conditioned at selected initial temperatures (T_0), ranging from −54 °C to 71 °C.

5.1 Infrared (IR) microscopy
The propellant grain was placed onto an adhesive, cut by a microtome into thin slices (thickness 7 µm) and analyzed by IR microscopy. A Bruker Hyperion

infrared microscope mounted on a Vector 33 Fourier-transform spectrometer was used. A medium-band MCT (HgCdTe) detector in the microscope gives high sensitivity in the 4000-600 cm^{-1} range. A 15X cassegrain mirror objective was used to obtain the infrared spectra. The IR spectrometer was operated at a resolution of 4 cm^{-1} and 32 scans were acquired for each measurement position. The measuring window had an aperture of 10 μm × 50 μm, the longer side of the aperture being placed perpendicular to the measured diameter. The increment for each data point was 3 μm. The DBP concentration was obtained by using the ratio of two IR bands, one typical of DBP (1720 cm^{-1}), one typical of nitrocellulose (1160 cm^{-1}).

5.2 Closed vessel tests

The closed vessel experiments were performed in a vessel of volume 118 cm^3. The tests were performed at different initial temperatures (−54 °C, 21 °C and 71 °C).

   Before temperature conditioning, the propellant was placed in a closed glass bottle. This bottle was then conditioned for at least 8 h before the test, in an oven for conditioning at higher temperatures or in a Lauda thermostatic bath for conditioning at lower temperatures, and then tested immediately, within ≯30 s, after being removed from the conditioning cabinet. The closed vessel was loaded with the conditioned propellant at the initial temperature T_0 and the test was performed as soon as possible. The test was carried out at ambient temperature, *i.e.* the closed vessel was at ambient temperature and the propellant was at the initial temperature. It was assumed that the temperature change in the propellant during the time between removal from the conditioning facility and ignition of the propellant was negligible. The propellant loading density was 0.15 g/cm^3. Pressures were recorded using a piezo-electric transducer Kistler 6215. The output voltage of the pressure sensor was transmitted to a data acquisition system at a sampling rate of 250 kHz. The propellant charges were ignited using a gaseous ignition mixture. The gaseous ignition system consisted of two electrodes, which were connected with the filament and a valve to introduce methane (CH$_4$) and oxygen (O$_2$). The partial pressures (0.1 MPa of CH$_4$ and 0.14 MPa of O$_2$) were measured with a piezo-electric pressure transducer (Kistler 4070). The filament connecting the two electrodes ignited the gas mixture by the Joule effect, when an electric current was passed.

   A typical output from a closed vessel test was the pressure history and, after post-test processing, the burning rate. A computer program provided both the smoothed curve P = f (t) [Gaussian smoothing was used, which is a method of digital smoothing allowing the elimination of the dispersion and oscillations of

the pressure time data without affecting the characteristics of the signal (maxima, minima, slope *etc.*)], and calculated its derivative dP/dt.

The burning rate was obtained according to STANAG 4115 by the product of three terms. Two terms are based on the form function and on the differentiation of a modified Noble-Abel equation, respectively. The third term is the derivative of the pressure obtained, as explained above.

6 Results

6.1 Deterrent concentration profile

Figure 1 represents the deterrent concentration profile obtained by IR microscopy measurements. The vertical dashed lines limit the three parts of the investigated propellant. The penetration depth was, for the first part between 0 µm and 23 µm, for the second part between 23 µm and 60 µm, and for the last part greater than 60 µm.

In order to determine the corresponding pressures limiting the combustion of the various parts of the propellant, the variation of the penetration depth as a function of the pressure is shown in Figure 2. It was observed that 23 µm and 60 µm were equivalent to pressures equal to 41 MPa and 90 MPa, respectively.
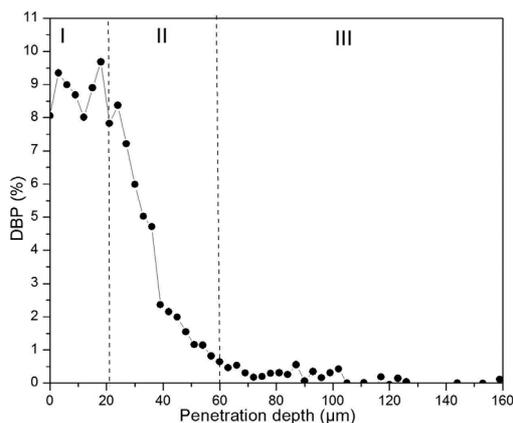

Figure 1. Deterrent concentration profile of the spherical propellant measured by infrared microscopy
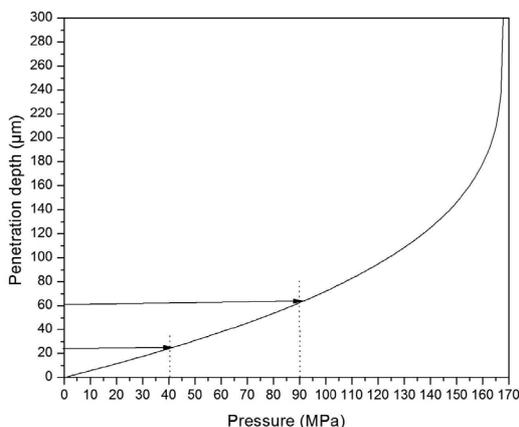
Figure 2.   Penetration depth as a function of pressure

6.2 Pressure inside the closed vessel

Figure 3 shows the pressure time profile from a closed vessel test obtained at ambient temperature. It may be observed that the maximal realized pressure is equal to 167 MPa. Note that this is independent of the initial temperature of the propellant. The maximal pressure reached by the ignition system alone inside the closed vessel was equal to 4.68 MPa [2], which represents only 3% of the maximal pressure obtained by testing the propellant. The range of pressures where the ignition system has an influence was eliminated. In fact, the burning rate was investigated only between 20% and 70% of the maximal pressure inside the closed vessel [3].
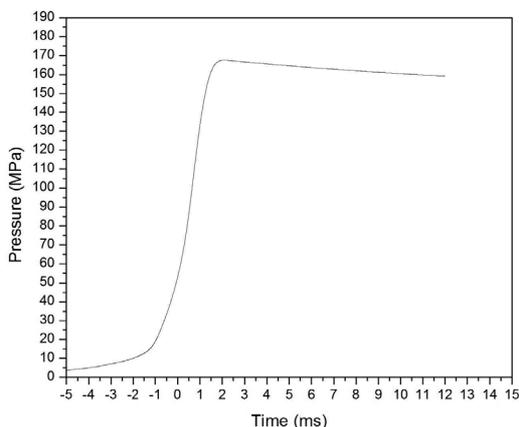
Figure 3.   Pressure time profile from a closed vessel test

6.3 Burning rate

The variation of the burning rate as a function of the pressure is shown in Figure 4. Based on the previously obtained values of pressure (Section 6.1) obtained from the three parts of the propellant, we identify three zones of combustion of the propellant in the burning rate law, illustrated by the two vertical dashed lines (Figure 4). These two vertical lines illustrate the range of pressures where the burning rate was investigated (between 20% and 70% of the maximal pressure inside the closed vessel).
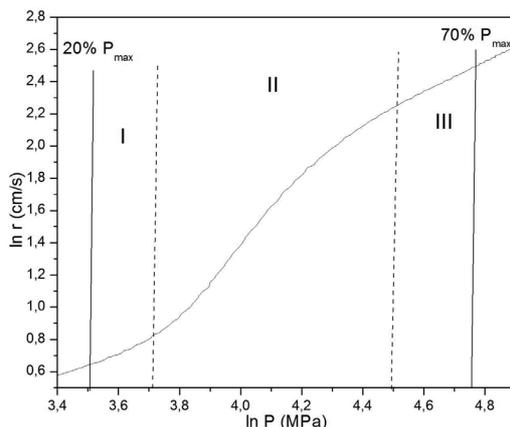
Figure 4. Variation of the burning rate as a function of the pressure at $T_0 = 21$ °C. The vertical lines limit the zones of combustion of the three parts of the propellant
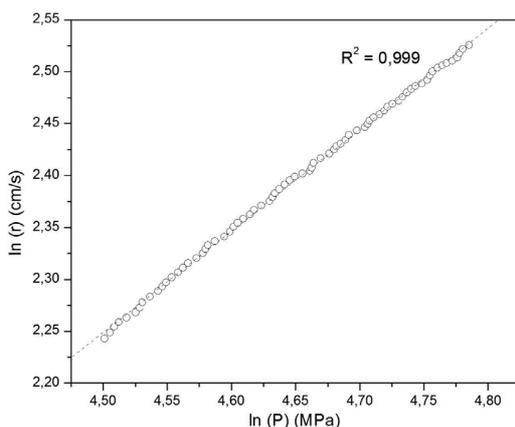
6.3.1 Deterred part of the propellant

Figure 5 represents the curve of $\ln r$ versus $\ln P$ of the first (I) part of the propellant. It may be observed that the variation of $\ln r$ versus $\ln P$ exhibits good linearity, meaning that Vieille's law $r_P = \beta \cdot P^\alpha$ is appropriate to describe the variation of the burning rate of the deterred part of the propellant as a function of pressure in this particular pressure range. Indeed, the correlation coefficient of linearity (R^2) was equal to 0.997.
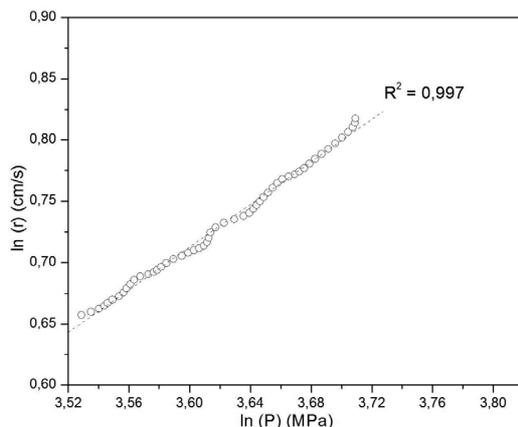
Figure 5. $\ln r$ versus $\ln P$ curve of the deterred part of the spherical propellant ($T_0 = 21$ °C). The dashed line represents the linear regression

6.3.2 Undeterred part of the propellant

Figure 6 represents the curve of $\ln r$ versus $\ln P$ of the third (III) part of the propellant. It may be noticed that the variation of $\ln r$ versus $\ln P$ exhibits good linearity, meaning that Vieille's law $r_P = \beta \cdot P^\alpha$ is adequate to describe the variation of the burning rate of the undeterred part of the propellant as a function of pressure. In fact, the correlation coefficient of linearity (R^2) was equal to 0.999.

Figure 6. $\ln r$ versus $\ln P$ curve of the undeterred part of the spherical propellant ($T_0 = 21$ °C). The dashed line represents the linear regression

6.4 Temperature sensitivity coefficient $\sigma\,(r_P)$

After we had identified where the combustion of the three parts of the propellant occurs, we calculated the temperature sensitivity coefficient $\sigma\,(r_P)$ corresponding to the first and third parts, in order to determine $\sigma\,(r_P)$ of the deterred and the undeterred parts of the propellant, respectively.
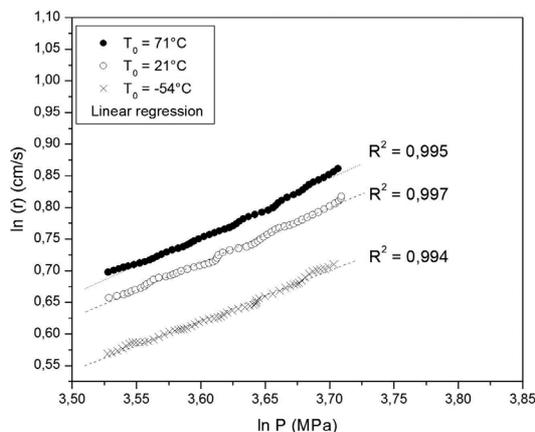
6.4.1 Deterred part of the propellant

The assumption that, in the traditional Vielle's law, $r_P = \beta \cdot P^\alpha$, the pressure exponent, α, is not a function of the initial temperature, corresponds to the assumption that the slope of $\ln(r)$ versus $\ln(P)$ resulting from different initial temperatures remains constant. As illustrated in Figure 7, this assumption appears to be reasonable. Consequently, the temperature sensitivity coefficient $\sigma\,(r_P)$ of the deterred part of the propellant is independent of pressure; this is listed in Table 2.

Consequently we calculated that, for the investigated spherical propellant, the temperature sensitivity coefficient $\sigma\,(r_P)$ of the deterred part was equal to:

- 0.083%/°C (towards high temperatures),
- 0.125%/°C (towards low temperatures).

Table 2. Values of the temperature sensitivity coefficient ($\sigma\,(r_P)$) of the deterred part of the spherical propellant at various pressures. Values in brackets are *one* standard deviation in %

| $\ln(P)$ [MPa]	$\sigma\,(r_P)$ [%/°C]	
	71 °C/21 °C	21 °C/−54 °C
3.55	0.079	0,115
3.57	0.078	0.121
3.62	0.072	0.132
3.67	0.091	0.128
3.71	0.094	0.127
Average	0.083 (±11 %)	0.125 (±4 %)

Figure 7. Temperature dependence of the $\ln r$ versus $\ln P$ curve of the deterred part of the spherical propellant. The dashed lines represent the linear regressions

6.4.2 Undeterred part of the propellant

As for the deterred part of the propellant, the assumption that, in the traditional Vielle's law, $r_P = \beta \cdot P^\alpha$, the pressure exponent, α, is not a function of the initial temperature appears to be reasonable (Figure 8, Table 3). The temperature sensitivity coefficient $\sigma(r_P)$ of the undeterred part was found to be equal to:

- 0.092%/°C (towards high temperatures),
- 0.072%/°C (towards low temperatures).
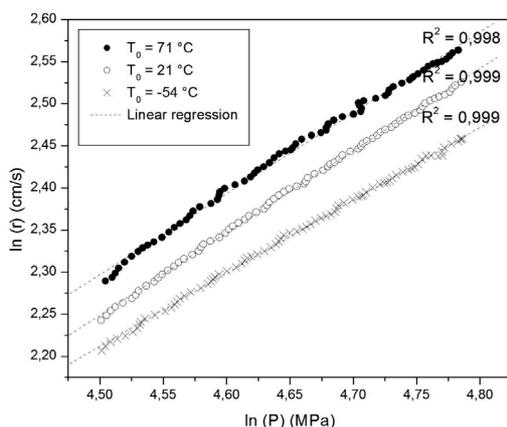
Figure 8. Temperature dependence of the $\ln r$ versus $\ln P$ curve of the undeterred part of the spherical propellant. The dashed lines represent the linear regressions

Table 3. Values of the temperature sensitivity coefficient ($\sigma\,(r_P)$) of the undeterred part of the spherical propellant at various pressures. Values in brackets are *one* standard deviation in %

Pressure [MPa]	$\sigma\,(r_P)$ [%/°C]	
	71 °C/21 °C	21 °C/−54 °C
4.52	0.100	0.059
4.57	0.093	0.059
4.62	0.093	0.066
4.67	0.090	0.080
4.77	0.086	0.096
Average	0.092 (±5%)	0.072 (±13%)

6.4.3 Discussion

We observed that for the deterred part of the propellant the values of the temperature sensitivity coefficients increased from 0.083%/°C (towards high temperatures) to 0.125%/°C (towards low temperatures), and for the undeterred part of the propellant, the values of the temperature sensitivity coefficients decreased from 0.092%/°C to 0.072%/°C, respectively. This indicates that the chemical composition influences the temperature sensitivity of the propellant.

7   Conclusions

This paper demonstrates an experimental procedure that allows the local temperature sensitivity coefficients $\sigma(r_P)$ of a deterred spherical single base gun propellant to be determined.

Initially, we measured the deterrent concentration profile of the investigated spherical deterred propellant in order to locate the various parts of the propellant. In fact, there are three parts; the first zone corresponds to the deterred portion of the propellant grain where the concentration of DBP is largest, the second zone is the portion where the DBP content is lower, and the third zone contains no DBP.

Subsequently, it has been shown that for the chemically homogenous parts of the propellant (the first and the last parts), the variation of the burning rate as a function of pressure can be described adequately by the Vielle law. In fact the temperature sensitivity coefficients $\sigma(r_P)$ of the deterred and undeterred parts of the deterred spherical gun propellant corresponds to $\sigma\,(r_P)$ of the first and third zones, respectively.

For the deterred part of the propellant, we found the temperature sensitivity coefficients $\sigma(r_P)$ were equal to 0.083%/°C (towards high temperatures) and 0.125%/°C (towards low temperatures).

For the undeterred part of the propellant, towards high temperatures $\sigma(r_P)$ is equal to 0.092%/°C, and towards low temperatures $\sigma(r_P)$ is equal to 0.072%/°C.

References

[1] Boulkadid, M. K.; Lefebvre, M. H.; Jeunieau, L.; Dejeaifve, A. Temperature Sensitivity of Propellant Combustion and Temperature Coefficients of Gun Performance. *Cent. Eur. J. Energ. Mater.* **2016**, *13*(4): 1005-1022.

[2] Jeunieau, L.; Lefebvre, M. H.; Guillaume, P. Characterization of Deterred Propellants by Closed Vessel Tests: Importance of the Ignition Method. *Cent. Eur. J. Energ. Mater.* **2005**, *2*: 39-53.

[3] Assovskii, G.; Zakirov, Z. G.; Leipunskii, O. I. Effect of Ignition on Fuel Combustion. *Combust., Expl., Shock Waves (Engl. Transl.)* **1983**, *19*(1): 37-41.

[4] Leciejewski, Z.; Surma, Z. Effect of Application of Various Ignition Conditions in Closed Vessel Tests on Burning Rate Calculation of a Fine-grained Propellant. *Combust., Expl. Shock Waves (Engl. Transl.)* **2011**, *47*(2): 209-216.

[5] Woodley, C.; Taylor, M.; Wheal, H. Boundary Layer Modelling of the Heat Transfer Process from Igniters to Energetic Materials. *Proc. 23rd Int Symp. on Ballistics*, Vol. I, Tarragona, Spain **2007**, 295-302.

[6] Khristenko, Yu. F. Experimental Methods for Studying the Combustion of Granular Powder in a Broad Range of Process Parameters. *Combust., Expl., Shock Waves (Engl. Transl.)* **2001**, *27*(1): 72-77.

[7] *Definition and Determination of Ballistic Properties of Gun Propellants.* STANAG 4115, North Atlantic Council, **1997**.

[8] Fong, C. W. *Temperature Sensitivity of Aircraft Cannon Propellants*. AFATLTR-82-72, Eglin Airforce Base, FL, Air Force Armament Laboratory, **1982**.

[9] Nguyen, T. T.; Spear R. J. *Approaches to Reducing the Temperature Sensitivity of Propulsion Systems for Artillery Ammunition*. DSTO Aeronautical and Maritime Research Laboratory, AR No. 008-974, Australia **1994**.

[10] Jeunieau, L.; Lefebvre, M. H.; Dejeaifve, A.; Dobson, R.; Fonder, N. Sensitivity of Nitrocellulose Propellants to the Firing Temperature. *5th Int. Symposium on Energetic Materials and their Applications*, Fukuoka, Japan, 12-14 November, **2014**.

[11] Jeunieau, L.; Lefebvre, M. H.; Dejeaifve, A.; Fonder, N.; Guillaume, P.; Boukfessa, H. Centralite Deterred Ball Powder Propellant: Stability and Influence of the Firing Temperature. *2013 Int. Autumn Seminar on Propellants, Explosives and Pyrotechnics*, 24-27 September, Chengu, China **2013**.

[12] Jeunieau, L.; Lefebvre, M. H.; Guillaume, P.; Fonder, N. Ballistic Stability and

Influence of the Firing Temperature on Deterred Propellants. *2nd Int. Symposium on High Energy Materials*, Incheon, South Korea, 17-20 September, **2012**.

[13] Jeunieau, L.; Lefebvre, M. H.; Guillaume, P. Ballistic Stability and Influence of the Firing Temperature of Two Deterred Propellants. *5th Int. Nitrocellulose Symposium*, Spiez, Switzerland, 17-18 April, **2012**.

[14] Oberle, W.; White, K. *The Application of Electrothermal-Chemical (ETC) Propulsion Concepts to Reduce Propelling Charge Temperature Sensitivity*. ARL-TR-1509, U.S. Army Ballistic Research Laboratory, Aberdeen Proving Ground, MD, **1997**.

[15] Clifford, W.; Bertram, K. *Ballistic Criteria for Propellant Grain Fracture in the GAU-8/A 30 MM Gun*. AFATL-TR-82-21, **1982**.

[16] Jeunieau, L.; Lefebvre, M. H.; Guillaume, P. Quantitative Infra-Red Microscopy Method for the Determination of the Deterrent Diffusion Activation Energy in a Spherical Propellant. *Cent. Eur. J. Energ. Mater.* **2007**, *4*: 109-124.